Rainfall-Soil Moisture Event Responses near Baton Rouge, Louisiana

Ali Haghighi (ahaghighi@ut.ac.ir), Afshin Ashrafzadeh (a.ashrafzadeh@ut.ac.ir) September 28, 2025

1 Introduction

Rainfall governs soil moisture variability and drives hydrological processes from infiltration to contaminant transport. This study provides a concise, high-level analysis of event-scale rainfall–soil moisture interactions near Baton Rouge, Louisiana, during 2022–2024. We identify individual rainfall events, quantify their soil moisture responses, and highlight the interplay among pre-event soil moisture, post-event soil moisture, soil moisture change ($\Delta\theta$), and event precipitation. The framework has potential for future expansion to incorporate nitrate leaching and surface-subsurface contamination analysis.

Resources: Codes and processed data (spatially and temporally subsampled; easy-to-use CSV) are available on GitHub repository. My personal website and other projects can be found at Ciarel.com.

2 Study Area and Data

The analysis domain is a 25 × 25 km box surrounding Baton Rouge, Louisiana (SW: 30.34, -91.28; NE: 30.56, -91.02), as shown in Fig. 1. This bounding box was chosen to capture regional hydroclimatic variability while maintaining a tractable spatial scale for event-based soil moisture analysis. Both precipitation and soil moisture datasets were subsetted spatially to this domain and temporally to the period 2022–2024.

Figure 1: Study area near Baton Rouge, Louisiana. The analysis domain (25 × 25 km box) is outlined and overlain on regional context.

Soil moisture conditions were obtained from the NASA Soil Moisture Active Passive (SMAP) mission, using the Enhanced Level-3 Radiometer Global Daily product (9 km resolution), which provides surface soil moisture retrievals representative of the top ∼5 cm of soil [1]. Precipitation data were obtained from the Global Precipitation Measurement (GPM) mission's Integrated Multi-satellite Retrievals (IMERG) Final Run product, available at 0.1° spatial and daily temporal resolution [2].

Together, SMAP and IMERG provide harmonized, global-scale, open-access satellite observations suitable for characterizing - moisture interactions in regions such as Baton Rouge, where high-frequency precipitation events and strong seasonal cycles affect vadose-zone hydrology.

3 Methods

Rainfall events were defined from daily precipitation P_t. A wet day is $P_t \geq 1$ mm, and an event is a sequence of wet days that (i) starts after a dry day, and (ii) includes a burst of at least 5 mm on the first or second day. For an event with start s and end e, total rainfall and duration are

$$R = \sum_{t=s}^{e} P_t, \qquad D = e - s + 1.$$

Pre-event soil moisture is the mean of the three days before the event, but if these overlap with the previous event, we trim them. Let A denote this window and θ_A its average. The post-event response window is

$$B = \big[s,\ \min(e+3,\ s_{\text{next}} - 1)\big], \qquad \theta_{\max} = \max_{t \in B} \theta_t.$$

The main metric is the soil moisture increment

$$\Delta\theta = \theta_{\max} - \theta_A.$$

We also compute a nominal lag between pre-event soil moisture and response times. However, we do not analyze it further because SMAP provides only surface soil moisture (∼0–5 cm) at daily resolution. With no information from deeper layers, infiltration timing and true lags cannot be extracted reliably. If multi-depth soil measurements were available, lag analysis would be a valuable extension.

4 Results

Hydroclimatic context. Monthly precipitation and domain-mean soil moisture (Fig. 2) track each other closely, with wetter months yielding higher soil moisture. Peaks occur at the end of winter and early spring, reflecting cumulative cool-season rainfall and low evaporative demand.

Rainfall events. Event characteristics are shown in Fig. 3. The median event produced 25 mm over 2 days. High-depth, long-duration outliers (above the 75th percentile in both) occurred mainly in summer. Seasonal counts were Winter 31, Spring 31, Summer 29, and Autumn 23.

Soil moisture responses. For each rainfall event, the soil moisture increment ($\Delta\theta$) was calculated. Fig. 4 shows representative cases, highlighting how soil moisture responds to multi-day storms while smaller events are sometimes undetected by the event definition. Aggregated results across all events are summarized in Fig. 5. The panels illustrate how $\Delta\theta$, pre-event soil moisture, post-event soil moisture, and event precipitation interact. A clear saturation boundary emerges: high pre-event moisture constrains additional gains, whereas drier conditions allow increases up to 18%. Seasonal clustering reflects this—winter and spring events occur near saturation, while summer and autumn cover a broader, drier range. Looking at the distributions of pre- and post-event soil moisture (top boxplots), a clear shift toward higher values is evident: while the overall range remains similar, the distribution skews toward the upper bound (≈45%), and the post-event median even exceeds the pre-event 75th percentile.

5 Future Research

Future research could extend this event-based framework by incorporating nitrate, deeper soil moisture, and aquifer data into a fully integrated modeling approach, as in Boujoudar et al. [3]. This would allow exploration of contamination transport and aquifer interaction in addition to rainfall-driven infiltration responses. Such analysis could also be highly valuable in regions with scarce rainfall, where farmers must rely on rainfall-soil moisture assessments and predictions for decision-making [4].

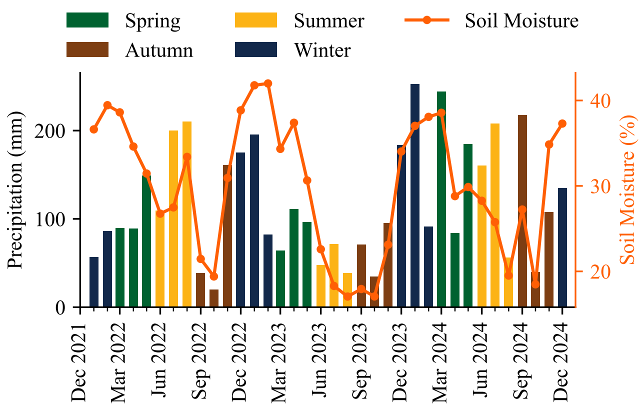

Figure 2: Monthly precipitation totals and averaged soil moisture from 2022-2024.

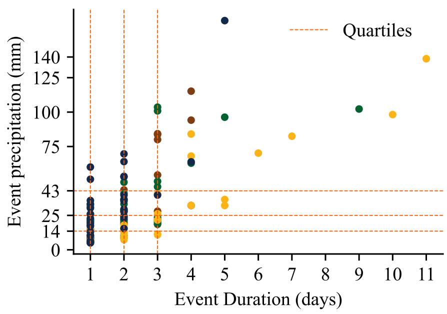

Figure 3: Event rainfall depth versus duration.

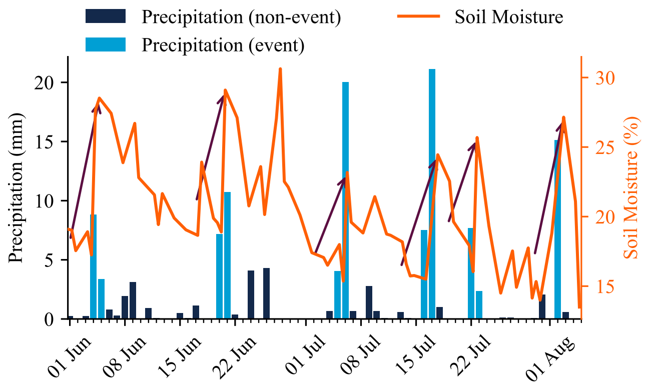

Figure 4: Example rainfall event: daily precipitation and soil moisture response.

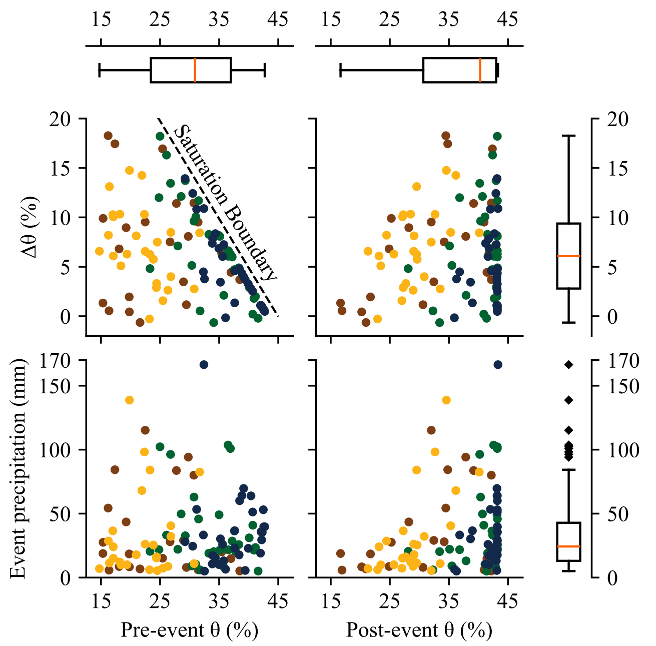

Figure 5: Relationships among pre-event soil moisture, post-event soil moisture, event precipitation, and soil moisture change ($\Delta\theta$), with distributions of each variable shown along the axes.

References

[1] P. E. O'Neill et al. *SMAP Enhanced L3 Radiometer Global and Polar Grid Daily 9 km EASE-Grid Soil Moisture, Version 6*. Subset: Baton Rouge, Louisiana, 2022–2024. Accessed 2025-09-27. Boulder, Colorado USA, 2021. DOI: 10.5067/M20OXIZHY3RJ. URL: https://nsidc.org/data/SPL3SMP_E.

[2] G. J. Huffman et al. *GPM IMERG Final Precipitation L3 1 day 0.1 degree × 0.1 degree V07 (GPM_3IMERGDF)*. Subset: Baton Rouge, Louisiana, 2022–2024. Accessed 2025-09-27. Greenbelt, Maryland, USA, 2023. DOI: 10.5067/GPM/IMERGDF/DAY/07. URL: https://data.nasa.gov/dataset/gpm-imerg-final-precipitation-l3-1-day-0-1-degree-x-0-1-degree-v07-gpm-3imergdf-at-ges-dis-13ed8.

[3] Mohamed Boujoudar et al. *Modeling Water, Heat, and Nitrate Dynamics in the VadoseZone: A Case Study of the Beauce Aquifer (Orleans, France)*. Tech. rep. Copernicus Meetings, 2025.

[4] Ali Haghighi, Masoud Parsinejad, and Javad Bazrafshan. "An Integrated Forecast-Simulation System for Intelligent Preseason Farming Decision Support". In: *Journal of Irrigation and Drainage Engineering* 151.6 (2025), p. 04025037.